Materials Science & Engineering C 108 (2020) 110415

Contents lists available at ScienceDirect

Materials Science & Engineering C

journal homepage: www.elsevier.com/locate/msec

Characterization of extracellular matrix modified poly(ε-caprolactone) electrospun scaffolds with differing fiber orientations for corneal stroma regeneration

Julia Fernández-Pérez[a,b,1], Karl E. Kador[a,b,c,1], Amy P. Lynch[a,b], Mark Ahearne[a,b,*]

[a] Trinity Centre for Biomedical Engineering, Trinity Biomedical Science Institute, Trinity College Dublin, the University of Dublin, Dublin, Ireland
[b] Department of Mechanical and Manufacturing, School of Engineering, Trinity College Dublin, the University of Dublin, Dublin, Ireland
[c] Department of Ophthalmology and Biomedical Sciences, University of Missouri-Kansas City, Kansas City, MO, USA

ARTICLE INFO

Keywords:
Cornea
Tissue engineering
Electrospinning
ECM

ABSTRACT

Alternatives to donor cornea transplantation based on tissue engineering are desirable to overcome the current severe donor tissue shortage. Many natural polymers have good biological properties but poor mechanical properties and degradation resistance; while synthetic polymers have good mechanical properties but do not contain biochemical molecules normally found in the real tissue. In addition, both fiber orientation and composition play a key role in dictating cell behavior within a scaffold. In this study, the effect on corneal stromal cells of adding decellularized corneal extracellular matrix (ECM) to an electrospun polymer with differing fiber organizations was explored. Electrospun matrices were generated using polycaprolactone (PCL) and PCL combined with ECM and electrospun into random, radial and perpendicularly aligned fiber scaffolds. Human corneal stromal cells were seeded onto these scaffolds and the effect of composition and orientation on the cells phenotype was assessed. Incorporation of ECM into PCL increased hydrophilicity of scaffolds without an adverse effect on Young's modulus. Cells seeded on these matrices adopted different morphologies that followed the orientation of the fibers. Keratocyte markers were increased in all types of scaffolds compared to tissue culture plastic. Scaffolds with radial and perpendicularly aligned fibers promoted enhanced cell migration. Aligned scaffolds with incorporated ECM show promise for their use as cell-free implants that promote endogenous repopulation by neighboring cells.

1. Introduction

The cornea is the transparent outermost layer of the anterior eye whose primary responsibility is to focus light onto the lens where it is refracted onto the retina. The corneal stroma makes up 90% of the corneal thickness and consists of keratocytes and collagen fibrils in a collagen/proteoglycan matrix [1,2]. Within the stroma, parallel collagen fibrils form lamellae that in turn are orientated orthogonally to each other [3]. The unique composition and structure is believed to be necessary for maintaining its health and optical properties [3,4]. Damage to the cornea from injury or disease can disrupt the stromal structure and lead to corneal opacity, one of the most common causes of blindness [5]. Keratoplasty, or corneal transplantation, is the gold standard procedure to treat corneal blindness: however, corneal blindness is still a major problem due to a shortage of healthy donor corneas suitable for transplantation [6–8]. For this reason, alternative solutions are under investigation.

One approach to overcome the shortage of donor corneas is to develop biomaterial scaffolds that mimic the cornea. Scaffolds manufactured from collagen type 1, the most abundant protein in the cornea, have been extensively investigated for replacing and regenerating the corneal stroma [9–11]. While these scaffolds have good transparency and can support the growth of keratocytes and epithelial cells, they often exhibit inferior mechanical strength and stiffness compared to the native tissue [12,13]. In addition, the use of collagen type 1 alone to generate a scaffold may not be sufficient for maintaining a normal native keratocyte phenotype [14]. The various collagen subtypes and proteoglycans within the corneal ECM are believed to be necessary for regulating normal keratocyte behavior and supporting the cells to maintain the cornea's ECM and transparency [15,16]. To more

* Corresponding author at: Trinity Centre for Biomedical Engineering, Trinity Biomedical Sciences Institute, 152-160 Pearse Street, Trinity College Dublin, Dublin 2, Ireland.
E-mail address: ahearnm@tcd.ie (M. Ahearne).
[1] T0hese authors contributed equally to this manuscript.

https://doi.org/10.1016/j.msec.2019.110415
Received 31 August 2018; Received in revised form 8 November 2019; Accepted 9 November 2019
Available online 11 November 2019

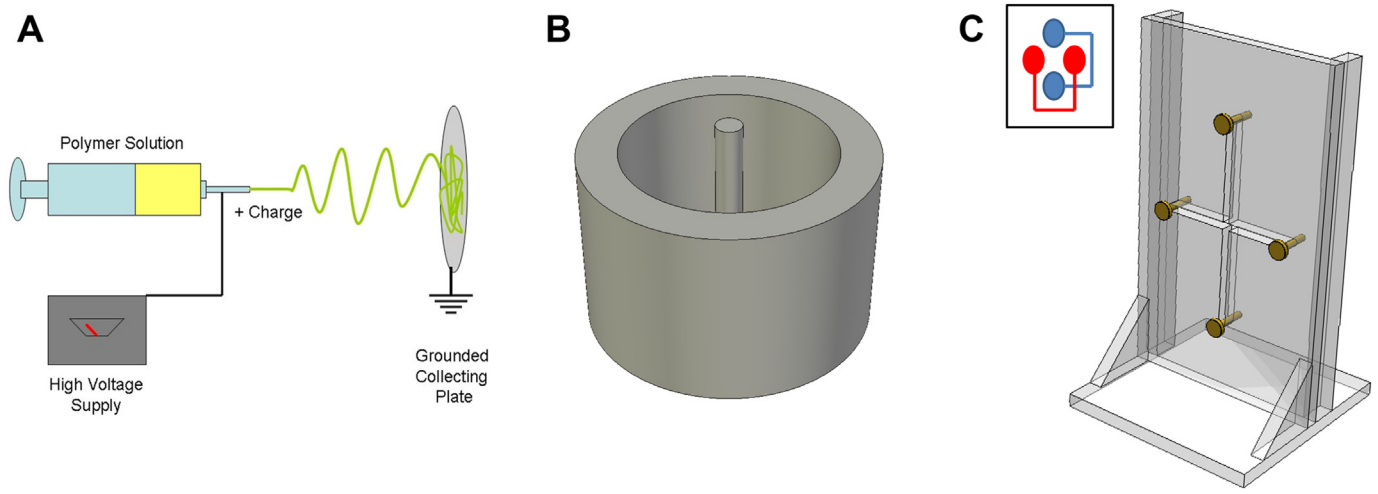

Fig. 1. Schematics of the production of aligned scaffolds. (A) General electrospinning process, (B) collector used for radially aligned scaffolds and (C) collector used for perpendicularly aligned scaffolds, inset depicts the horizontal and vertical wiring.

accurately mimic the composition of the cornea, acellular scaffolds manufactured from decellularized stromal tissue have been examined [17–20]. While these retain the composition and structure of the native corneal stroma, difficulty remains in trying to recellularize the scaffolds. Hydrogels manufactured from decellularized corneal ECM have also been explored [21,22]. Despite cells embedded in ECM hydrogels demonstrating an increased expression of keratocyte markers when compared to cells in collagen hydrogels [21], these scaffolds still lack control over the fiber organization.

Electrospinning is a widely utilized technique to create scaffolds with nanoscale or microscale diameter fibers using natural or synthetic polymers. The polymer is dissolved in a suitable solvent and placed into a syringe attached to a needle. A high voltage power supply applies an electric charge to the needle. As the solution is extruded though the needle, the electric charge passes through the polymer solution causing fibers to be formed in a whipping motion and these fibers can be collected on a grounded or negatively charged collector. When using a plate collector, the scaffolds form a random fibrous network; however, by using specific collectors, scaffolds can be created with uniaxial aligned [23–25], radially aligned [26,27] or perpendicularly aligned fiber orientations [28]. Several studies have shown that fiber orientation can direct cell migration and proliferation [29] and influence cell metabolic activity [25] and phenotype [30]. Natural polymers such as collagen or gelatin have been examined for use in electrospinning; however, they generally have poor mechanical properties and limited degradation resistance unless subjected to harsh cross-linking treatments [31]. Synthetic biocompatible polymers such as poly(ε-caprolactone) (PCL), poly(L-lactic acid) (PLLA) or poly(glycolic acid) (PGA) have previously been examined for generating aligned scaffolds [32,33]; however, they lack the ECM components needed to accurately replicate the native tissue.

The aim of this study was to determine the effect that different scaffold properties have on regulating corneal stromal cell behavior. Specifically, the influence of fiber orientation and the addition of ECM molecules were evaluated. This information is vital in determining the optimal fabrication conditions needed to generate scaffolds for corneal tissue engineering.

2. Materials and methods

2.1. Materials

Purasorb PC12 PCL pellets were a generous donation from Corbion. 1,1,1,3,3,3 hexafluoroispropanol (HFIP) was purchased from Fluorochem Limited. Low glucose Dulbecco modified eagle's medium (DMEM), penicillin and streptomycin solution (Pen/Strep) and GlutaMax were purchased from Life Technologies. Fibroblast growth factor-2 was purchased from RnD Systems. DNAse, RNAse, fetal bovine serum (FBS), L-ascorbic acid-2-phosphate, phalloidin-TRITC, DAPI, Triton-X100 and chloroform were purchased from Sigma-Aldrich. Advanced DMEM, Trizol and all TaqMan probes were purchased from ThermoFisher Scientific. High capacity cDNA reverse transcription kits were purchased from Invitrogen. Sylgard 184 PDMS was purchased from Farnell Ireland Limited. Fresh porcine eyes were obtained from a local butchers, within 12 h of sacrifice.

2.2. Methods

2.2.1. Corneal decellularization

Corneas were decellularized as previously described using freeze thaw cycling [21]. Briefly, fresh porcine corneas were dissected within 12 h of sacrifice using a 1 cm biopsy punch from the center. Corneas were placed in deionized water (3 ml/cornea) and frozen at a temperature of −80 °C for a minimum of 4 h and then thawed at room temperature. Once thawed the water was exchanged and the freeze thaw cycle was repeated for 5 cycles. Following the final wash, the corneas were incubated with 10 U/ml DNAse and 10 U/ml RNAse for 1 h at 37 °C to remove any residual nucleic acids and then washed in deionized water at room temperature for 72 h with rotation and the water exchanged every 24 h. Corneas were frozen at −80 °C and lyophilized for 24 h at −30 °C and 200 mbar. The freeze dried corneas were then milled to form a fine ECM powder using a Spex 6770 cryomill.

2.2.2. Scaffold fabrication

Scaffolds were prepared by overnight rotational mixing using either a polymer solution of 10% (w/v) PCL in HFIP or a 9% PCL + 1% ECM powder in HFIP. The solutions were loaded into a glass syringe with a 22 gauge needle and placed into a syringe pump. The collector was positioned in front of the syringe pump, 12 cm from the needle tip and a voltage of 15 kV applied to the needle. A feed rate of 2 ml/h at room temperature was used for all scaffolds. The process was carried out at temperatures ranging from 24 to 28 °C and at a humidity between 30 and 40%, similar to that previously reported [34].

Different collectors were used to generate different fiber orientations within the scaffolds (Fig. 1). To generate a random architecture, a standard microscope slide wrapped in aluminum foil and attached to a ground was used. Electrospun fibers were deposited for 15 min per

slide, with individual samples cut from the fiber mat using a 1 cm biopsy punch. To generate a radial architecture, a cup and pin collector described previously was used [26]. Briefly, a plastic cup 1.8 cm in diameter was covered in aluminum, and copper wire placed through the cup center with the central pin and aluminum grounded to the same source. Samples were deposited with 100–200 µl of solution. To generate perpendicularly oriented fibers, a collector was constructed as previously described [28]. 1 cm diameter electrodes were arranged in a vertical cross with the two electrodes on the vertical and the two electrodes on the horizontal separated by approximately 4 cm and with the two on the vertical and the two on the horizontal tied together electrically. A high voltage power source of opposite charge to that used to charge the syringe was passed through a G25 high voltage switch (Gigavac) and used to move a negative 7–10 kV charge between the horizontal and vertical electrodes throughout the electrospinning process with a switching rate of 15 s. Samples were created using 300 µl of solution and non-specific fibers which formed around the periphery were cut away from the sample.

2.2.3. FTIR analysis

Random fiber samples of PCL and PCL/ECM fibers were analyzed by attenuated total reflectance Fourier transform infrared spectrometer (Perkin Elmer Spectrum-100). Spectra from 4000 cm^{-1} to 650 cm^{-1} with 4 cm^{-1} resolution were analyzed for 80 scans with peaks analyzed and assigned using the Spectrum software.

2.2.4. Mechanical characterization of scaffolds

Mechanical analysis was performed as described previously [34]. Briefly, 5 cm long aligned electrospun fiber bundles with 1 cm diameter random fiber region at each base for clamping were constructed from PCL and PCL/ECM using the two vertical electrodes of the perpendicular collector. Samples were soaked in PBS for 20 min and then mounted into a Zwick/Roell model Z2 twin column mechanical analyzer equipped with a 200 N load cell and using custom made serrated clamps lined with sandpaper. Digital images were then taken to determine the width of the sample. Thickness of the scaffolds was determined using an outside micrometer (Mitutoyo, Japan). Samples were loaded at a constant rate of 5 mm/min along the direction of the fiber alignment and the Young's modulus calculated from the stress/strain curve measured in the elastic region of the samples (n = 6).

2.2.5. Contact angle

Water contact angle for PCL fibers with and without ECM was calculated using an FTA125 (First Ten Angstroms, Inc.) setup and FTA32 software. Ultrapure water (18 Ω, deionized) was added to a 1 ml gastight Hamilton syringe and placed directly above sample. Using the FTA32 software, a video capture is initiated and a single drop of water released. Once the drop reached a static position, the angle of the drop to surface was measured. 3 samples each from two different preparations for each material were measured in 3 places.

2.2.6. SEM analysis

Electrospun samples were mounted and sputter coated with a gold/palladium mixture. Samples were then imaged under high vacuum using a Zeiss Ultra Plus Scanning Electron Microscope at 2 kV and at magnifications ranging from 200× to 5000×. Fiber orientation was calculated using the Directionality ImageJ plugin. Fiber thickness measurements were taken from SEM images at 5000× magnification. Calculations were based measuring a minimum of 10 fibers from three different images using ImageJ's measuring tool.

2.2.7. Corneal stromal cell culture

Primary corneal stromal cells were isolated from freshly dissected corneal rims as previously described [35] in accordance with the Declaration of Helsinki. Cells were expanded in low glucose DMEM supplemented with 10% FBS and 100 U/ml Pen/Strep and passaged or cryopreserved at 70% confluence. Cells for experimentation were used at passages 4 or 5. Once seeded for experiments, cells were cultured in a defined medium consisting of Advanced DMEM supplemented with 100 U/ml Pen/Strep, 2 mM GlutaMax, 0.1 mM L-ascorbic acid-2-phosphate and 10 ng/ml FGF-2. Samples were cultured for 7 days with media changes every third day.

2.2.8. Immunostaining

Following 7 days in culture in defined media, samples were fixed for 30 min and washed 3 times with PBS for 5 min each. Samples were blocked with 10% goat serum in PBS containing 0.2% Triton-X100. Phalloidin-TRITC (1:1000) was incubated overnight at 4 °C. Samples were washed once with PBS for 5 min and then incubated for 15 min with DAPI (1:2500 in PBS) followed by two 5-minute washes with PBS. Samples were stored in PBS at 4 °C until imaged using a Leica SP8 confocal microscope. Cell nuclei were counted using ImageJ to quantify cell number on scaffolds in each architecture.

Non-seeded radial PCL/ECM scaffolds were fixed and blocked as stated above. Samples were then incubated overnight at 4 °C with primary antibody to detect unaltered collagen type I at a concentration of 1:400 (ab90395, Abcam). Three 5-minute washes with PBS were performed and then incubation with a biotinylated secondary antibody was carried out, overnight at 4 °C (1:200, B7151, Sigma). Samples were then washed 3 times in PBS for 5 min each and ExtrAvidin-FITC (E2761, Sigma) diluted 1:100 was incubated for 90 min at room temperature, in the dark, followed by three 5-minute washes with PBS Samples were then imaged using a Leica SP8 confocal microscope.

2.2.9. Quantitative PCR

After 7 days in culture in defined media, samples were washed with cold sterile PBS and the RNA extracted using Trizol reagent with chloroform and isopropanol washes. Because of cell density, 3 samples were combined from each experiment to isolate the required level of RNA. cDNA templates were created using a high capacity cDNA reverse transcription kit. Quantitative PCR was conducted using TaqMan probes for ALDH3A1 (Hs00964880_m1), Collagen Type I (Hs00164004_m1), Smooth Muscle Actin (Hs00426835_g1) and glyceraldehyde-3-phosphate dehydrogenase (GAPDH, Hs02758991_g1). The data was analyzed using the $\Delta\Delta C_T$ method and expressed as a power of $2^{-\Delta\Delta CT}$. Samples from 3 independent experiments were compared with significance determined using a one-way ANOVA.

2.2.10. Cell migration

The following was performed in order to seed cells in a very confined space of known area. Sylgard 184 PDMS was cast as a sheet with a depth of 5 mm. 12 mm buttons were punched from the sheet using a biopsy punch and a 2 mm punch taken from the button. The PDMS button was placed above the electrospun scaffolds and weighted with a stainless steel washer to ensure contact. 2000 corneal keratocytes were seeded and allowed to attach for 24 h within the confines of the 2 mm punch. Following 24 h of culture, the PDMS button was removed and the samples cultured for an additional 24 h. Samples were fixed for 30 min and then stained with Phalloidin-TRITC as described above. Samples were imaged using a Leica SP8 confocal microscope and the total area of cell migration measured.

2.2.11. Statistics

All experiments were performed thrice using three replicates, unless otherwise stated. Statistical analyses were performed using GraphPad Prism Software 5.0 (GraphPad Software, Inc. La Jolla, CA). All data are presented as the mean ± standard deviation. Statistical significance was determined using one-way ANOVA with Tukey post-hoc analyses. Differences were considered to be statistically significant at $p \leq 0.05$.

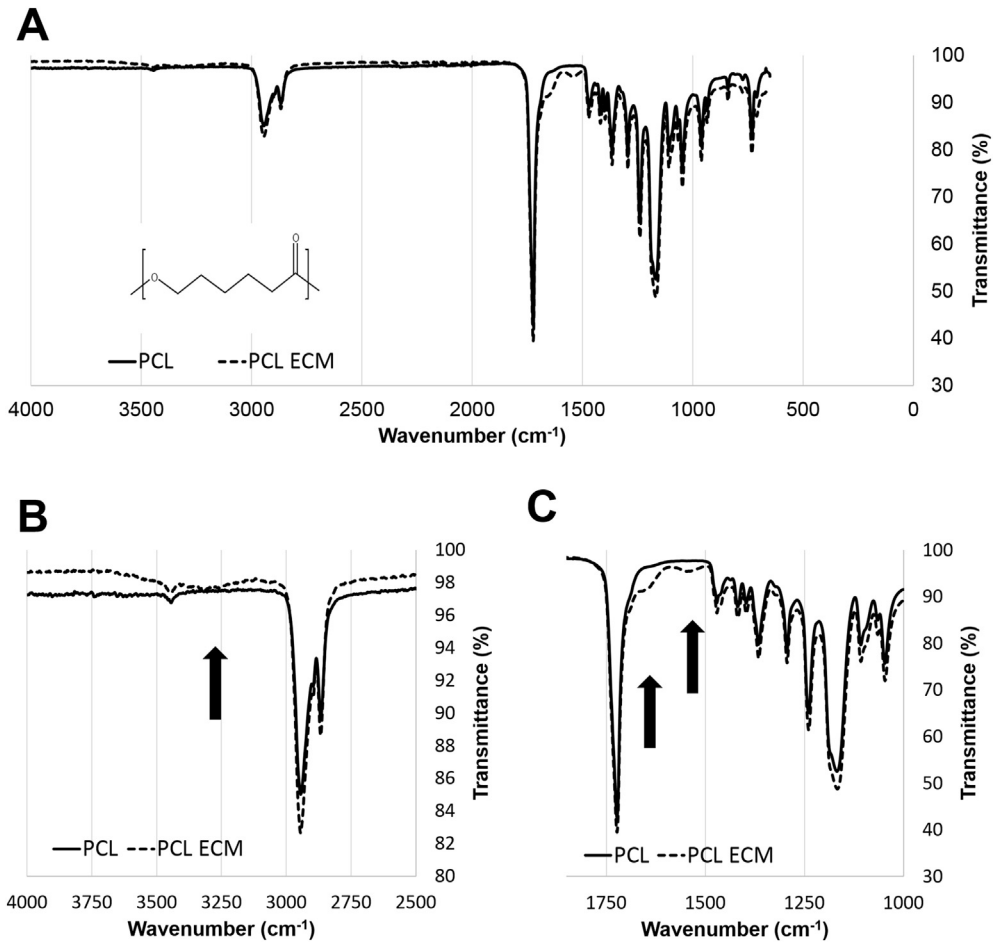

Fig. 2. Analysis of ECM incorporation. (A) FTIR analysis of scaffolds. New peaks were observed (B) at 3300 cm^{-1} corresponding to N—H stretch, (C) at 1660 cm^{-1} corresponding to a C═O stretch and at 1540 cm^{-1} corresponding to an N—H bend.

3. Results and discussion

3.1. Incorporation of ECM into electrospun fibers

Synthetic polymers such as PCL are commonly used for electrospinning for their excellent mechanical properties, even though generally these materials have less cell affinity than natural ones. Natural materials, such as collagen, can provide a better option due to their biocompatibility but these materials have fast degradation rates and lack mechanical strength [31]. Direct incorporation of ECM into PCL before electrospinning eliminated the need of cross-linking with toxic chemicals such as glutaraldehyde [36-38]. To confirm the presence of ECM components in PCL, FTIR was used (Fig. 2). Three new peaks were observed after the addition of ECM: one at 3300 cm^{-1} corresponding to N—H stretch (Fig. 2B); one at 1660 cm^{-1} corresponding to a C═O stretch; and one at 1540 cm^{-1} corresponding to a N—H bend (Fig. 2C) [39]. When taken together, this indicates the incorporation of amine and carboxyl functional groups found within peptide bonds into the PCL fibers with similar peaks having been found when combining PCL with collagen [40].

Previously, it has been reported that the electrospinning of collagen denatures the three dimensional structure of the protein resulting in the loss of mechanical properties as well as the loss of biological function [41]. However, other biological processes, such as specific cell binding domains, are independent of the three dimensional structure of collagen leading to the widespread use of gelatin within the electrospinning field. In this study, we used a non-detergent based method of decellularization to minimize denaturation of the ECM proteins and maximize retention of other ECM components such as sGAG [21]. Surprisingly, the presence of a distinct peak at 1660 cm^{-1} rather than a lower value of 1633 cm^{-1} indicates that collagen has not undergone substantive denaturation [42]. This was further confirmed by positive immunostaining for collagen type I in the scaffolds using an antibody that does not bind to denatured collagen (Fig. S1).

The incorporation of ECM into the PCL polymer before electrospinning did not have a detrimental effect on the mechanical characteristics of the scaffolds (Fig. 3). Uniaxial tensile tests revealed that there was no significant difference in the Young's modulus of the two types of scaffolds. PCL scaffolds had a Young's modulus of 9.76 MPa ± 2.27 MPa, while PCL/ECM constructs had a modulus of 9.20 MPa ± 2.63 MPa. These values are within previously reported ranges of Young's modulus (0.1 MPa to 57 MPa) for the human cornea [43]. Only the effect of material composition on the mechanical properties of the scaffolds was examined here, although fiber organization and the direction of applied strain relative to fiber orientation would also be expected to influence the modulus and strength [44, 45].

Other physical properties, such as the hydrophobicity of the scaffolds, were altered through the addition of ECM to PCL fibers (Fig. 4). Random fiber orientation scaffolds were produced from PCL and PCL/ECM and the hydrophobicity measured by water contact angle. Following the addition of ECM, the water contact angle was observed to decrease from 121.2° ± 2.0° for PCL scaffolds to 106.2° ± 8.4° for PCL/ECM scaffolds, suggesting a decrease in the hydrophobicity. By decreasing the hydrophobic nature of PCL, cell adhesion and growth on the fibers should be improved [46, 47].

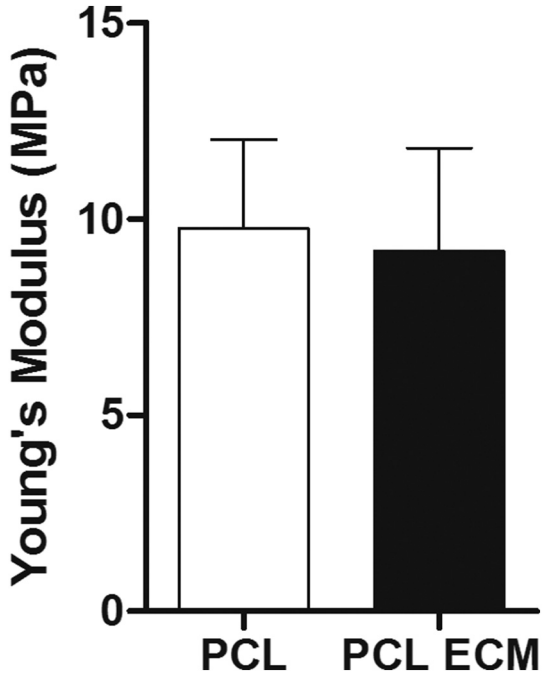

Fig. 3. Mechanical characterization of PCL and PCL/ECM scaffolds.

3.2. Scaffold architecture

Three different collectors were used to control the architecture of electrospun fibers and the arrangement of fibers within these scaffolds was confirmed via SEM (Fig. 5). As expected, fibers spun onto a flat collector had no specific orientation. Scaffolds generated using a pin and cup collectors consisted of radially aligned fibers running from the pin to the outer cup. Given that fibers are known to provide guidance cues to cells [26,27], this arrangement of fibers may be beneficial in allowing cells to migrate into the center from the outer edge, a migration pattern which is observed in corneal epithelial cell maintenance and wound healing. This orientation could be particularly useful if designing an acellular implant that wants to promote cell infiltration. The perpendicularly switching collectors allowed scaffolds with perpendicularly aligned fibers to be fabricated. The advantage of perpendicularly aligned fibers is that they more accurately replicate the fibril structure in the native corneal stroma, which consists of aligned fibrils that form layers that are orientated orthogonally to each other [48]. The switching collector is able to stack layers of aligned fibers orthogonally on top of each other by controlling the switching rate of the electrical potential on the collector. This method is advantageous compared to previously reported methods, which have generally required individual layers of aligned fibers to be manually assembled layer on layer [49,50].

Directionality analysis confirmed the expected fiber orientations in electrospun scaffolds. On randomly aligned scaffolds no fiber direction was predominant; while for the radially aligned scaffolds, fibers were mainly aligned in a single direction when a small region was examined. Unlike with parallel fibers such as the ones described by Olvera and colleagues [51], the histogram is wider indicating that the fibers are not parallel but rather originate from the same point and end separately. The distance from the center point and size of the area being examined will influence the orientation values. Two peaks separated by 90° appear for the perpendicularly aligned scaffolds. The larger peak represents the fibers on the top layer of the scaffold. Similar results were obtained when the PCL/ECM scaffolds were imaged and analyzed. The analysis of fiber thickness of the PCL only scaffolds showed that randomly aligned scaffolds had slightly thicker fibers (0.22 μm ± 0.05 μm) than the radial (0.20 μm ± 0.04 μm) and perpendicular (0.20 μm ± 0.06 μm) architectures. PCL/ECM scaffolds from random architecture had an average fiber size of was 0.20 μm ± 0.07 μm. Radial PCL/ECM scaffolds had an average fiber size of 0.18 ± 0.06 μm. Finally, perpendicular PCL/ECM scaffolds presented a fiber thickness with an average of 0.17 μm ± 0.04 μm. Fibers from all architectures had thicknesses ranging from 0.09 μm to 0.40 μm, which are considered microfibers.

3.3. Cell response to scaffolds

The addition of ECM to the scaffolds appeared to influence the morphology of cells (Fig. 6). Cells on randomly electrospun PCL fibers presented a rounded cell shape while on random PCL/ECM scaffolds, cells stretched along the fibers, displaying a predominantly elongated morphology with some small processes. Cells cultured on radially aligned PCL extended along a single fiber only, while on PCL/ECM scaffolds cells presented processes on multiple fibers. On perpendicularly aligned scaffolds, cells aligned mainly on the direction of one fiber, but often bridged onto orthogonal strands. Incorporation of ECM onto the perpendicularly aligned matrices enhanced this phenomenon. The differences in hydrophobicity and the presence of additional binding sites in PCL/ECM scaffolds compared to PCL scaffolds would explain these cell morphologies. Keratocytes in a healthy cornea stroma have a dendritic morphology [52]. Furthermore, for each orientation, the incorporation of ECM into PCL lead to a statistically significant increase in cell number when compared to scaffolds constructed from PCL only. In addition, there was a significantly increased number of cells found on scaffolds constructed of both radial and perpendicular architecture when compared to randomly oriented scaffolds (Fig. S2). The increase in cell number could be due to the ECM providing binding sites leading to an increased cell attachment during seeding or could be

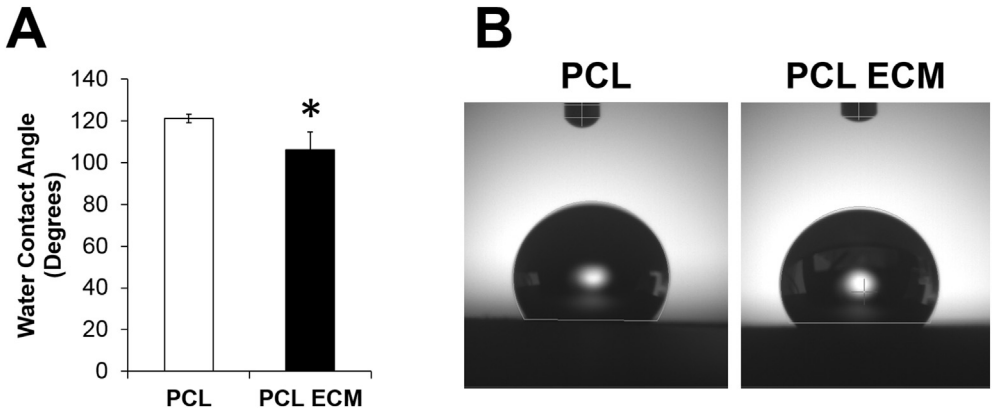

Fig. 4. Hydrophilicity analysis of scaffolds. (A) Quantitative and (B) macroscopic images depicting water contact angle of scaffolds. *p ≤ 0.05.

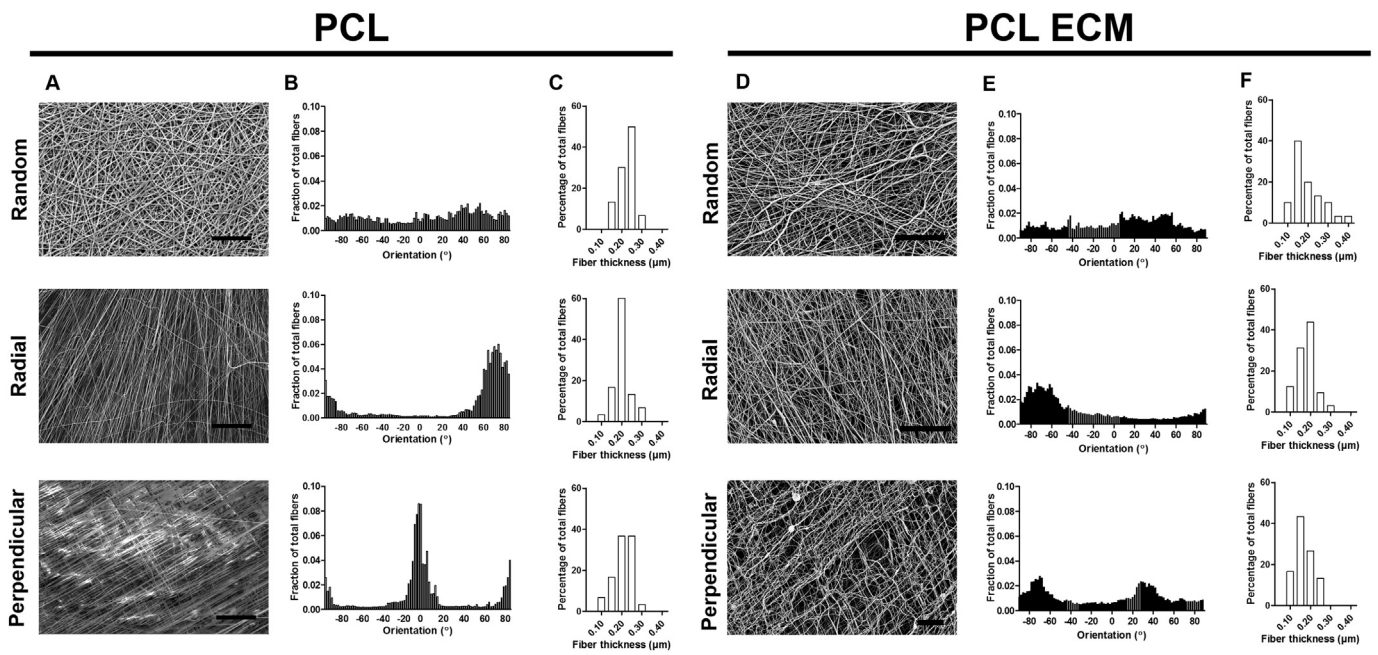

Fig. 5. Ultrastructure of PCL and PCL/ECM scaffolds. (A) SEM images; (B) quantification of fiber orientation and (C) quantification of fiber size of the PCL electrospun scaffolds; (D) SEM images; (E) quantification of fiber orientation and (F) quantification of fiber size of the PCL/ECM electrospun scaffolds. Scale bar = 25 μm.

due to the ECM stimulating an increase in proliferation of the stromal cells during culture. As is commonly observed, cells cultured on the different electrospun scaffolds did not migrate fully through the scaffold, instead seeding only onto the first 1–2 layers of fibers. While this allowed the keratocytes to be influenced by different fiber organizations, it would be a drawback to the creation of a full thickness tissue engineered construct. Currently different methods, such as the incorporation of sacrificial fibers to the scaffold [53] and the electrospraying of cells [54] into the scaffold during the electrospinning process, are being studied to overcome this limitation. However, they would need to be studied for their compatibility with the different collectors used to produce the scaffolds.

Gene expression analysis of cells on scaffolds showed that while orientation had a significant effect on ALDH3A1 expression, the additional ECM to PCL had no effect (Fig. 7). Cells on perpendicularly orientated scaffolds expressed less ALDH3A1 than those on random or radial scaffolds. ALDH3A1 is a corneal crystalline and commonly used as a marker of a keratocyte phenotype. Expression of collagen type 1

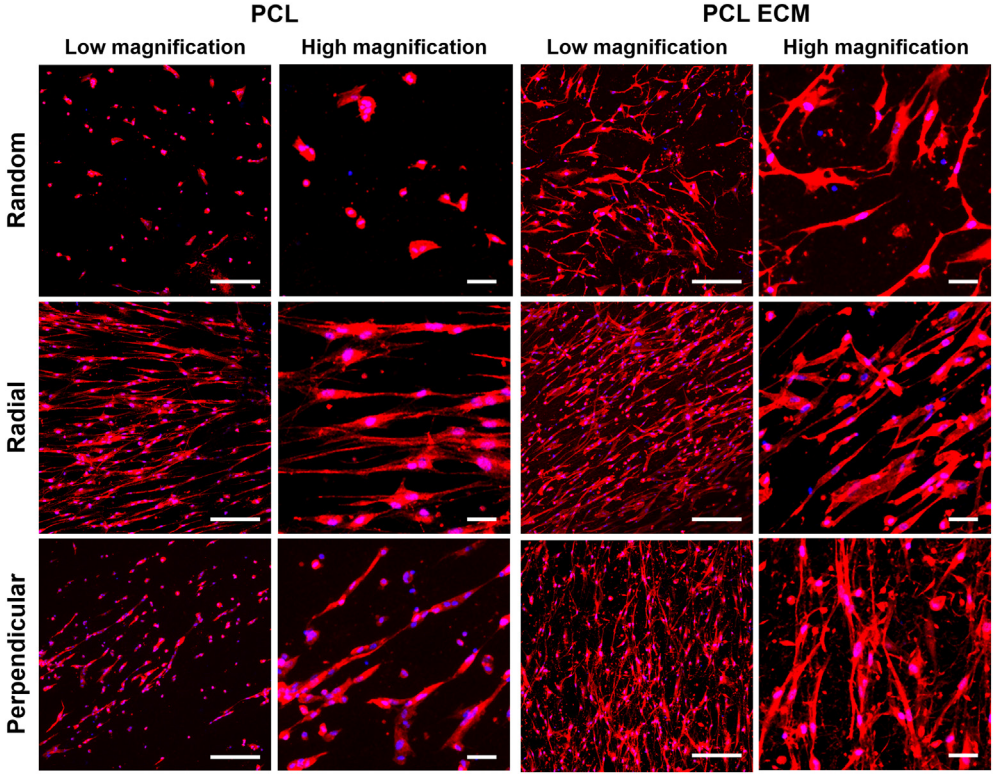

Fig. 6. Influence of fiber architecture and presence of ECM on keratocyte morphology. Cytochemical staining of seeded cells after 7 days in culture (blue = nuclei, red = F-actin; low magnification scale bar = 250 μm, high magnification scale bar = 50 μm). (For interpretation of the references to colour in this figure legend, the reader is referred to the web version of this article.)

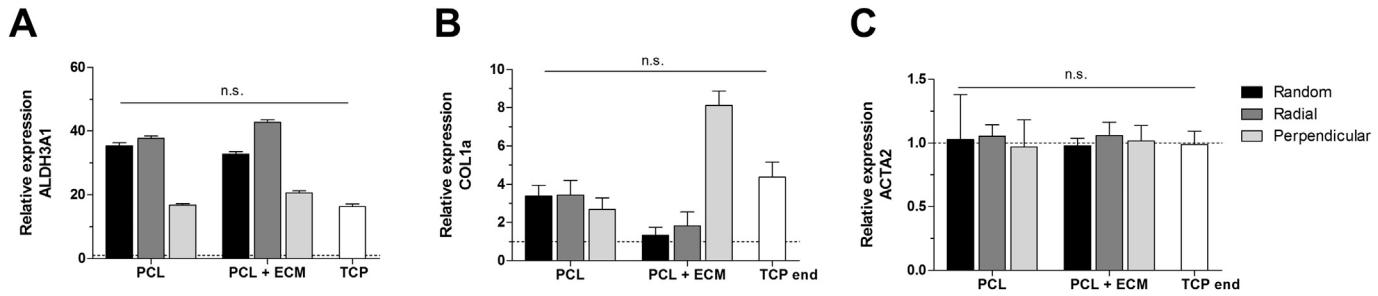

Fig. 7. Influence of fiber architecture and presence of ECM on keratocyte phenotype. Gene expression of (A) ALDH3A1, (B) COL1A and (C) ACTA2 (samples from 4 to 6 independent experiments, dashed line indicates level of expression of cells at the beginning of the experiment).

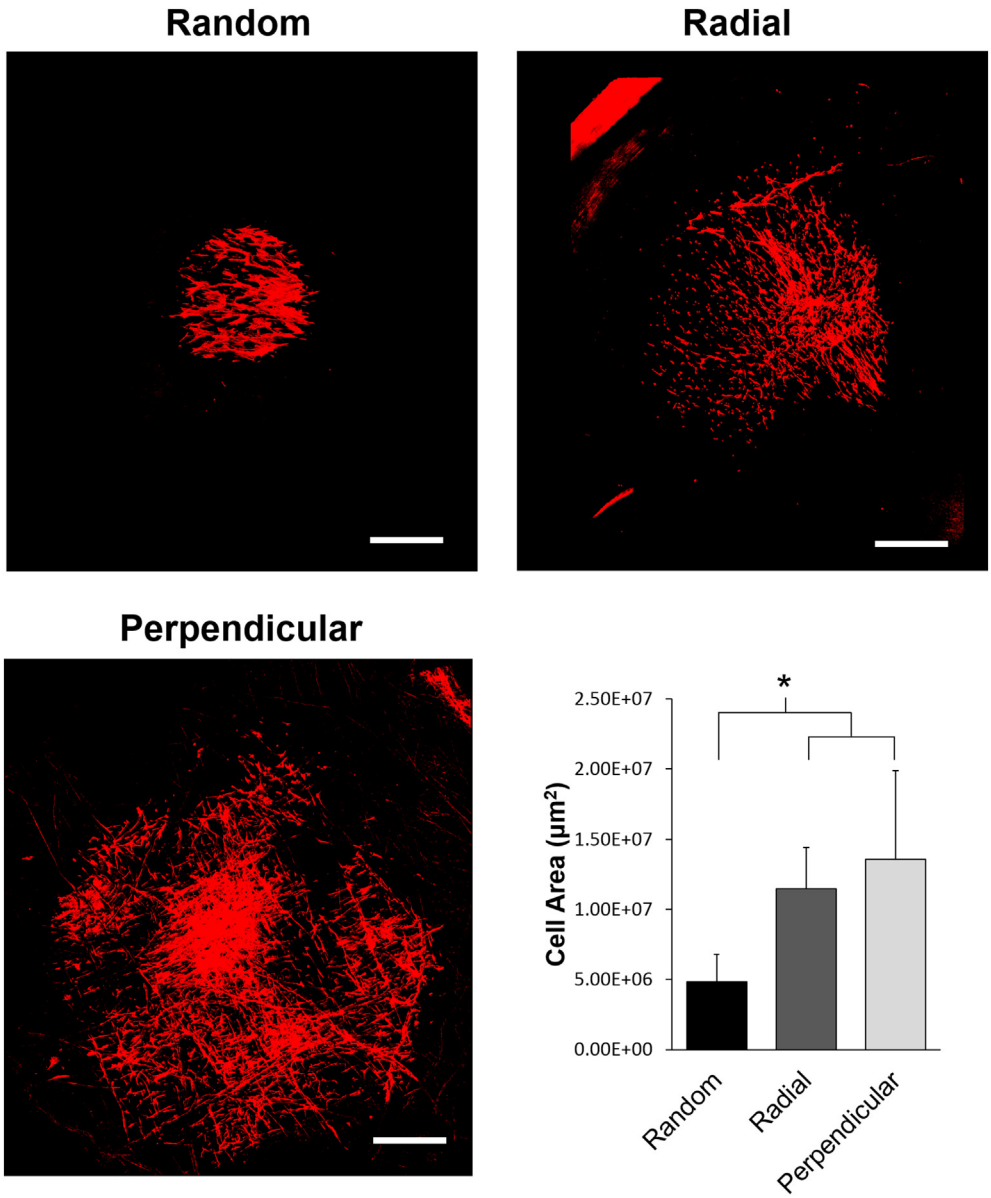

Fig. 8. Effect of fiber architecture on cell migration. Area occupied by cells after 24 h of culture on scaffolds, after initial seeding surface of 3×10^6 µm^2 (red = F-actin; scale bar = 1 mm; * $p \leq 0.05$). (For interpretation of the references to colour in this figure legend, the reader is referred to the web version of this article.)

was higher from cells on the PCL scaffolds with random and radial architectures than cells on PCL/ECM scaffolds with the same architectures. The opposite was true for cells on perpendicular scaffolds with PCL/ECM perpendicular scaffolds presenting the highest collagen type 1 expression of all groups. None of the scaffolds promoted the transformation of cultured cells into myofibroblasts, as there was no significant up-regulation of ACTA2, the gene for α-smooth muscle actin (α-SMA). Wray and Orwin reported a downregulation of α-SMA when rabbit corneal stromal cells were cultured on aligned collagen nanofibers in the presence of serum, which was not added in our study [55].

Other authors have shown upregulation of keratocyte markers on aligned substrates but only after long periods of culture (> 6 weeks) [56, 57].

To study cell migration, cells were seeded at the center of each scaffold with a confined seeding area of 3×10^6 μm^2. After 48 h, 24 h with the mask in place and 24 h with it removed to allow for cell migration, the cells were fixed, stained for actin and the area covered with cells was measured via confocal imaging (Fig. 8). On randomly aligned scaffolds, the cells covered an area of 4.86×10^6 μm^2 ± 1.93×10^6 μm^2 while cells on radial and perpendicularly aligned matrices covered a significantly greater area (11.46×10^6 μm^2 ± 2.96×10^6 μm^2 and 14.01×10^6 μm^2 ± 7.23×10^6 μm^2, respectively). This showed the increased migration capability of cells on scaffold with a defined alignment of electrospun fibers. These results, corroborate previous studies where cells seeded on aligned and radial scaffolds have shown an increase in migration rate when compared to randomly oriented fibers using other cell types [26, 58,59].

4. Conclusion

The influence on corneal stromal cells of fiber orientation and addition of corneal ECM to PCL fibers was demonstrated. Fiber alignment and ECM incorporation affected cells morphology but had no significant impact of phenotype. Cells aligned along electrospun fibers and extended processes along multiple fibers. Scaffolds with radial and perpendicularly aligned fibers promoted enhanced cell migration. This information will be useful for researchers developing next generation smart scaffolds for tissue regeneration.

Supplementary data to this article can be found online at https://doi.org/10.1016/j.msec.2019.110415.

Acknowledgements

The research leading to these results has received funding from the European Research Council (ERC) under the European Union's Horizon 2020 research and innovation program (grant agreement no. 637460) and from Science Foundation Ireland (15/ERC/3269).

Declaration of competing interest

None.

References

[1] A.J. Quantock, R.D. Young, Development of the corneal stroma, and the collagen-proteoglycan associations that help define its structure and function, Dev. Dyn. 237 (2008) 2607–2621, https://doi.org/10.1002/dvdy.21579.
[2] J.M. Fitch, J. Gross, R. Mayne, B. Johnson-Wint, T.F. Linsenmayer, Organization of collagen types I and V in the embryonic chicken cornea: monoclonal antibody studies, Proc. Natl. Acad. Sci. U. S. A. 81 (1984) 2791–2795.
[3] D.M. Maurice, The structure and transparency of the cornea, J. Physiol. 136 (1957) 263–286.
[4] K.M. Meek, C. Knupp, Corneal structure and transparency, Prog. Retin. Eye Res. 49 (2015) 1–16, https://doi.org/10.1016/j.preteyeres.2015.07.001.
[5] D. Robaei, S. Watson, Corneal blindness: a global problem, Clin. Exp. Ophthalmol. 42 (2014) 213–214, https://doi.org/10.1111/ceo.12330.
[6] D. Pascolini, S.P. Mariotti, Global estimates of visual impairment: 2010, Br. J. Ophthalmol. 96 (2012) 614–618, https://doi.org/10.1136/bjophthalmol-2011-300539.
[7] J.P. Whitcher, M. Srinivasan, M.P. Upadhyay, Corneal blindness: a global perspective, Bull. World Health Organ. 79 (2001) 214–221.
[8] P. Gain, R. Jullienne, Z. He, M. Aldossary, S. Acquart, F. Cognasse, G. Thuret, Global survey of corneal transplantation and eye banking, JAMA Ophthalmol 134 (2016) 167–173, https://doi.org/10.1001/jamaophthalmol.2015.4776.
[9] C.E. Ghezzi, J. Rnjak-Kovacina, D.L. Kaplan, Corneal tissue engineering: recent advances and future perspectives, Tissue Eng. Part B. Rev. 21 (2015) 278–287, https://doi.org/10.1089/ten.TEB.2014.0397.
[10] M. Griffith, E.I. Alarcon, I. Brunette, Regenerative approaches for the cornea, J. Intern. Med. 280 (2016) 276–286, https://doi.org/10.1111/joim.12502.
[11] I. Brunette, C.J. Roberts, F. Vidal, M. Harissi-Dagher, J. Lachaine, H. Sheardown, G.M. Durr, S. Proulx, M. Griffith, Alternatives to eye bank native tissue for corneal stromal replacement, Prog. Retin. Eye Res. 59 (2017) 97–130, https://doi.org/10.1016/j.preteyeres.2017.04.002.
[12] W. Liu, K. Merrett, M. Griffith, P. Fagerholm, S. Dravida, B. Heyne, J.C. Scaiano, M.A. Watsky, N. Shinozaki, N. Lagali, R. Munger, F. Li, Recombinant human collagen for tissue engineered corneal substitutes, Biomaterials 29 (2008) 1147–1158, https://doi.org/10.1016/j.biomaterials.2007.11.011.
[13] M. Ahearne, K.-K. Liu, A.J. El Haj, K.Y. Then, S. Rauz, Y. Yang, Online monitoring of the mechanical behavior of collagen hydrogels: influence of corneal fibroblasts on elastic modulus, Tissue Eng. Part C. Methods. 16 (2010) 319–327, https://doi.org/10.1089/ten.TEC.2008.0650.
[14] B.L. Farrugia, M.S. Lord, J.M. Whitelock, J. Melrose, Harnessing chondroitin sulphate in composite scaffolds to direct progenitor and stem cell function for tissue repair, Biomater. Sci. 6 (2018) 947–957, https://doi.org/10.1039/C7BM01158J.
[15] J.R. Hassell, D.E. Birk, The molecular basis of corneal transparency, Exp. Eye Res. 91 (2010) 326–335, https://doi.org/10.1016/j.exer.2010.06.021.
[16] J.-Y. Lai, Y.-T. Li, C.-H. Cho, T.-C. Yu, Nanoscale modification of porous gelatin scaffolds with chondroitin sulfate for corneal stromal tissue engineering, Int. J. Nanomedicine 7 (2012) 1101–1114, https://doi.org/10.2147/IJN.S28753.
[17] A.P. Lynch, S.L. Wilson, M. Ahearne, Dextran preserves native corneal structure during decellularization, Tissue Eng. Part C Methods. 22 (2016) 561–572, https://doi.org/10.1089/ten.tec.2016.0017.
[18] S.L. Wilson, L.E. Sidney, S.E. Dunphy, H.S. Dua, A. Hopkinson, Corneal decellularization: a method of recycling unsuitable donor tissue for clinical translation? Curr. Eye Res. 41 (2016) 769–782, https://doi.org/10.3109/02713683.2015.1062114.
[19] Y. Hashimoto, S. Funamoto, S. Sasaki, T. Honda, S. Hattori, K. Nam, T. Kimura, M. Mochizuki, T. Fujisato, H. Kobayashi, A. Kishida, Preparation and characterization of decellularized cornea using high-hydrostatic pressurization for corneal tissue engineering, Biomaterials 31 (2010) 3941–3948, https://doi.org/10.1016/j.biomaterials.2010.01.122.
[20] Q. Li, H. Wang, Z. Dai, Y. Cao, C. Jin, Preparation and biomechanical properties of an acellular porcine corneal stroma, Cornea 36 (2017) 1343–1351, https://doi.org/10.1097/ICO.0000000000001319.
[21] M. Ahearne, A.P. Lynch, Early observation of extracellular matrix-derived hydrogels for corneal stroma regeneration, Tissue Eng. Part C Methods. 21 (2015) 1059–1069, https://doi.org/10.1089/ten.tec.2015.0008.
[22] M. Ahearne, A. Coyle, Application of UVA-riboflavin crosslinking to enhance the mechanical properties of extracellular matrix derived hydrogels, J. Mech. Behav. Biomed. Mater. 54 (2016) 259–267, https://doi.org/10.1016/j.jmbbm.2015.09.035.
[23] D. Dippold, A. Cai, M. Hardt, A.R. Boccaccini, R. Horch, J.P. Beier, D.W. Schubert, Novel approach towards aligned PCL-collagen nanofibrous constructs from a benign solvent system, Mater. Sci. Eng. C. 72 (2017) 278–283, https://doi.org/10.1016/j.msec.2016.11.045.
[24] F. Yang, R. Murugan, S. Wang, S. Ramakrishna, Electrospinning of nano/micro scale poly(l-lactic acid) aligned fibers and their potential in neural tissue engineering, Biomaterials 26 (2005) 2603–2610, https://doi.org/10.1016/j.biomaterials.2004.06.051.
[25] P. Stafiej, F. Küng, D. Thieme, M. Czugala, F.E. Kruse, D.W. Schubert, T.A. Fuchsluger, Adhesion and metabolic activity of human corneal cells on PCL based nanofiber matrices, Mater. Sci. Eng. C. 71 (2017) 764–770, https://doi.org/10.1016/j.msec.2016.10.058.
[26] K.E. Kador, R.B. Montero, P. Venugopalan, J. Hertz, A.N. Zindell, D.A. Valenzuela, M.S. Uddin, E.B. Lavik, K.J. Muller, F.M. Andreopoulos, J.L. Goldberg, Tissue engineering the retinal ganglion cell nerve fiber layer, Biomaterials 34 (2013) 4242–4250, https://doi.org/10.1016/j.biomaterials.2013.02.027.
[27] J. Xie, M.R. MacEwan, W.Z. Ray, W. Liu, D.Y. Siewe, Y. Xia, Radially aligned, electrospun nanofibers as dural substitutes for wound closure and tissue regeneration applications, ACS Nano 4 (2010) 5027–5036, https://doi.org/10.1021/nn101554u.
[28] R.B. Montero, X. Vial, D.T. Nguyen, S. Farhand, M. Reardon, S.M. Pham, G. Tsechpenakis, F.M. Andreopoulos, BFGF-containing electrospun gelatin scaffolds with controlled nano-architectural features for directed angiogenesis, Acta Biomater. 8 (2012) 1778–1791, https://doi.org/10.1016/j.actbio.2011.12.008.
[29] Y.M. Shin, M.M. Hohman, M.P. Brenner, G.C. Rutledge, Electrospinning: a whipping fluid jet generates submicron polymer fibers, Appl. Phys. Lett. 78 (2001) 1149–1151, https://doi.org/10.1063/1.1345798.
[30] Z. Yin, X. Chen, J.L. Chen, W.L. Shen, T.M. Hieu Nguyen, L. Gao, H.W. Ouyang, The regulation of tendon stem cell differentiation by the alignment of nanofibers, Biomaterials 31 (2010) 2163–2175, https://doi.org/10.1016/j.biomaterials.2009.11.083.
[31] M. Kharaziha, M. Nikkhah, S.-R. Shin, N. Annabi, N. Masoumi, A.K. Gaharwar, G. Camci-Unal, A. Khademhosseini, PGS:gelatin nanofibrous scaffolds with tunable mechanical and structural properties for engineering cardiac tissues, Biomaterials 34 (2013) 6355–6366, https://doi.org/10.1016/j.biomaterials.2013.04.045.
[32] C. Zhang, J. Wen, J. Yan, Y. Kao, Z. Ni, X. Cui, H. Wang, In situ growth induction of the corneal stroma cells using uniaxially aligned composite fibrous scaffolds, RSC Adv. 5 (2015) 12123–12130, https://doi.org/10.1039/C4RA16609D.
[33] S. Sharma, D. Gupta, S. Mohanty, M. Jassal, A.K. Agrawal, R. Tandon, Surface-modified electrospun poly(ε-caprolactone) scaffold with improved optical transparency and bioactivity for damaged ocular surface reconstruction, Investig. Opthalmology Vis. Sci. 55 (2014) 899, https://doi.org/10.1167/iovs.13-12727.
[34] D. Olvera, R. Schipani, B.N. Sathy, D.J. Kelly, Electrospinning of highly porous yet mechanically functional microfibrillar scaffolds at the human scale for ligament and tendon tissue engineering, Biomed. Mater. 14 (2019) 035016, , https://doi.org/10.1088/1748-605X/ab0de1.
[35] A.P. Lynch, F. O'Sullivan, M. Ahearne, The effect of growth factor supplementation

on corneal stromal cell phenotype in vitro using a serum-free media, Exp. Eye Res. 151 (2016) 26–37, https://doi.org/10.1016/j.exer.2016.07.015.
[36] D.P. Speer, M. Chvapil, C.D. Eskelson, J. Ulreich, Biological effects of residual glutaraldehyde in glutaraldehyde-tanned collagen biomaterials, J. Biomed. Mater. Res. 14 (1980) 753–764, https://doi.org/10.1002/jbm.820140607.
[37] L.L. Huang-Lee, D.T. Cheung, M.E. Nimni, Biochemical changes and cytotoxicity associated with the degradation of polymeric glutaraldehyde derived crosslinks, J. Biomed. Mater. Res. 24 (1990) 1185–1201, https://doi.org/10.1002/jbm.820240905.
[38] D.M. Simmons, J.N. Kearney, Evaluation of collagen cross-linking techniques for the stabilization of tissue matrices, Biotechnol. Appl. Biochem. 17 (Pt 1) (1993) 23–29.
[39] R.M. Silverstein, G.C. Bassler, T.C. Morrill, Spectrometric Identification of Organic Compounds, 5th ed., Wiley, 1991.
[40] V.Y. Chakrapani, A. Gnanamani, V.R. Giridev, M. Madhusoothanan, G. Sekaran, Electrospinning of type I collagen and PCL nanofibers using acetic acid, J. Appl. Polym. Sci. 125 (2012) 3221–3227, https://doi.org/10.1002/app.36504.
[41] D.I. Zeugolis, S.T. Khew, E.S.Y. Yew, A.K. Ekaputra, Y.W. Tong, L.Y.L. Yung, D.W. Hutmacher, C. Sheppard, M. Raghunath, Electro-spinning of pure collagen nano-fibres - just an expensive way to make gelatin? Biomaterials 29 (2008) 2293–2305, https://doi.org/10.1016/j.biomaterials.2008.02.009.
[42] K.J. Payne, A. Veis, Fourier transform IR spectroscopy of collagen and gelatin solutions: Deconvolution of the amide I band for conformational studies, Biopolymers 27 (1988) 1759–1760, https://doi.org/10.1002/bip.360271105.
[43] N. Garcia-Porta, P. Fernandes, A. Queiros, J. Salgado-Borges, M. Parafita-Mato, J.M. González-Méijome, Corneal biomechanical properties in different ocular conditions and new measurement techniques, ISRN Ophthalmol. 2014 (2014) 1–19, https://doi.org/10.1155/2014/724546.
[44] K. Tonsomboon, M.L. Oyen, Composite electrospun gelatin fiber-alginate gel scaffolds for mechanically robust tissue engineered cornea, J. Mech. Behav. Biomed. Mater. 21 (2013) 185–194, https://doi.org/10.1016/j.jmbbm.2013.03.001.
[45] D.G.T. Strange, K. Tonsomboon, M.L. Oyen, Mechanical behaviour of electrospun fibre-reinforced hydrogels, J. Mater. Sci. Mater. Med. 25 (2014) 681–690, https://doi.org/10.1007/s10856-013-5123-y.
[46] Y. Li, M. Ceylan, B. Shrestha, H. Wang, Q.R. Lu, R. Asmatulu, L. Yao, Nanofibers support oligodendrocyte precursor cell growth and function as a neuron-free model for myelination study, Biomacromolecules 15 (2014) 319–326, https://doi.org/10.1021/bm401558c.
[47] Y. Zhu, C. Gao, J. Shen, Surface modification of polycaprolactone with poly(methacrylic acid) and gelatin covalent immobilization for promoting its cytocompatibility, Biomaterials 23 (2002) 4889–4895, https://doi.org/10.1016/S0142-9612(02)00247-8.
[48] Y. Komai, T. Ushiki, The three-dimensional organisation of collagen fibrils in the human cornea and sclera, Investig. Ophthalmol. Vis. Sci. 32 (1991) 2244–2258.
[49] S.L. Wilson, I. Wimpenny, M. Ahearne, S. Rauz, A.J. El Haj, Y. Yang, Chemical and topographical effects on cell differentiation and matrix elasticity in a corneal stromal layer model, Adv. Funct. Mater. 22 (2012) 3641–3649, https://doi.org/10.1002/adfm.201200655.
[50] Y. Yang, I. Wimpenny, M. Ahearne, Portable nanofiber meshes dictate cell orientation throughout three-dimensional hydrogels, Nanomedicine Nanotechnology, Biol. Med. 7 (2011) 131–136, https://doi.org/10.1016/j.nano.2010.12.011.
[51] D. Olvera, B.N. Sathy, S.F. Carroll, D.J. Kelly, Modulating microfibrillar alignment and growth factor stimulation to regulate mesenchymal stem cell differentiation, Acta Biomater. 64 (2017) 148–160, https://doi.org/10.1016/J.ACTBIO.2017.10.010.
[52] C.A. Poole, N.H. Brookes, G.M. Clover, Confocal imaging of the human keratocyte network using the vital dye 5-chloromethylfluorescein diacetate, Clin. Exp. Ophthalmol. 31 (2003) 147–154, https://doi.org/10.1046/j.1442-9071.2003.00623.x.
[53] B.M. Baker, A.O. Gee, R.B. Metter, A.S. Nathan, R.A. Marklein, J.A. Burdick, R.L. Mauck, The potential to improve cell infiltration in composite fiber-aligned electrospun scaffolds by the selective removal of sacrificial fibers, Biomaterials 29 (2008) 2348–2358, https://doi.org/10.1016/J.BIOMATERIALS.2008.01.032.
[54] D. Braghirolli, P. Pranke, F. Zamboni, G.A.X. Acasigua, Association of electrospinning with electrospraying: a strategy to produce 3D scaffolds with incorporated stem cells for use in tissue engineering, Int. J. Nanomedicine 10 (2015) 5159, https://doi.org/10.2147/IJN.S84312.
[55] L.S. Wray, E.J. Orwin, Recreating the microenvironment of the native cornea for tissue engineering applications, Tissue Eng. Part A. 15 (2009) 1463–1472, https://doi.org/10.1089/ten.tea.2008.0239.
[56] J. Wu, Y. Du, S.C. Watkins, J.L. Funderburgh, W.R. Wagner, The engineering of organized human corneal tissue through the spatial guidance of corneal stromal stem cells, Biomaterials 33 (2012) 1343–1352, https://doi.org/10.1016/j.biomaterials.2011.10.055.
[57] J. Wu, Y. Du, M.M. Mann, E. Yang, J.L. Funderburgh, W.R. Wagner, Bioengineering organized, multilamellar human corneal stromal tissue by growth factor supplementation on highly aligned synthetic substrates, Tissue Eng. Part A. 19 (2013) 2063–2075, https://doi.org/10.1089/ten.TEA.2012.0545.
[58] K.E. Kador, S.P. Grogan, E.W. Dorthé, P. Venugopalan, M.F. Malek, J.L. Goldberg, D.D. D'lima, Control of retinal ganglion cell positioning and neurite growth: combining 3D printing with radial electrospun scaffolds, Tissue Eng. Part A. 22 (2016) 286–294, https://doi.org/10.1089/ten.tea.2015.0373.
[59] J.I. Kim, J.Y. Kim, C.H. Park, Fabrication of transparent hemispherical 3D nanofibrous scaffolds with radially aligned patterns via a novel electrospinning method, Sci. Rep. 8 (2018) 1–13, https://doi.org/10.1038/s41598-018-21618-0.